Stability of DC Distribution Systems: Analytical and Experimental Results

Nils H. van der Blij
Electrical Sustainable Energy
Delft University of Technology
Delft, The Netherlands
N.H.vanderBlij@TUDelft.nl

Laura M. Ramirez-Elizondo
Electrical Sustainable Energy
Delft University of Technology
Delft, The Netherlands
L.M.RamirezElizondo@TUDelft.nl

Matthijs T. J. Spaan
Software Technology
Delft University of Technology
Delft, The Netherlands
M.T.J.Spaan@TUDelft.nl

Wuhua Li
College of Electrical Engineering
Zhejiang University
Hangzhou, China
WoohuaLee@ZJU.edu.cn

Pavol Bauer
Electrical Sustainable Energy
Delft University of Technology
Delft, The Netherlands
P.Bauer@TUDelft.nl

***Abstract*—Constant power loads combined with low inertia form a major challenge for future distribution grids. This paper presents a state-space representation to model dc distribution systems. Two methods are discussed to analyze the (small-signal) stability of these dc distribution systems; an algebraic method and a Brayton-Moser method. The system models and the methods for stability analysis were verified using an experimental dc microgrid set-up. Furthermore, it was found that the instability of dc distribution systems can be classified into two categories: equilibrium instability and oscillatory instability.**

Keywords— dc distribution, eigenvalues, sensitivity analysis, stability, state-space

I. INTRODUCTION

Future distribution grids will be subjected to significant changes. Firstly, large scale renewable power generation will be situated in areas with high resource availability rather than high consumption [1]. Secondly, the introduction of decentralized generation causes the power flow in the system to no longer be unidirectional [2]. Lastly, with the increasing participation of renewable energy resources, the uncertainty in distribution system is increased. Moreover, because of the islanding of microgrids, not only supply and demand are subjected to uncertainty, but also the topology of the distribution grid is becoming uncertain [2]-[4]. Yet, it is critical that the availability, accessibility and safety of future distribution systems are ensured.

The application of dc distribution systems becomes appealing since they have several advantages compared to ac distribution systems. Primarily, dc distribution grids are foreseen to have advantages with regards to efficiency, control, distribution capacity, and converters [5], [6].

Adoption of dc distribution systems is expanding expeditiously. Utilization of dc systems for applications such as data centres, telecommunications, commercial and residential buildings and street lighting is growing [7], [8]. Furthermore, a variety of novel applications, such as microgrids and device level distribution, have been identified recently [9].

Stability for future (dc) distribution grids is more complex compared to conventional ac distribution grids. Firstly, with the increasing presence of power electronics and the increasing share of renewable energy the inertia in the grid is decreasing [10]. Secondly, constant power loads have a significant adverse effect on stability due to their negative incremental impedance [11]. Lastly, distribution grids are subjected to changes in grid topology, direction of power flow, and meshes [3].

Two common stabilization methods have been identified to ensure stability in dc distribution systems. Firstly, passive stabilization which utilizes passive elements to dampen disturbances in the system [12]. Secondly, active stabilization using advanced control methods [13]. However, it is more cost effective to ensure inherent stability in dc distribution systems, when possible.

In literature, four main approaches to analyse the stability of dc distribution systems can be found. Firstly, a root locus of the system can be drawn for the locations of the poles under changing system parameters [14]. However, this approach does not provide general insights into stability. Secondly, the relationship between load and source impedance, the minor loop gain, can be analysed [15]. However, unidirectional power flow is assumed and measurements are crucial for accurate impedance estimations. Thirdly, Lyapunov methods can be used to analyse stability [16]. However, finding and applying suitable Lyapunov storage functions is challenging. Lastly, the poles of the system can be derived from its state-space representation [17]. This method relies on the linearization of the system, and is also used in this paper.

Previous research analyses specific topologies, uses oversimplified models, or do not provide general rules for stability. In this paper a state-space representation for any dc distribution system, including its converters, is presented. From this representation methods to analyse the stability algebraically and ensure stability for plug-and-play systems are derived.

The main contribution of this paper is the experimental validation of the dc distribution system model, the stability analysis methods and their derived observations.

The remainder of this paper is organized as follows: in Section II a generic algebraic model of dc distribution systems is introduced. In Section III different methods to analyse the stability of dc distribution systems are discussed. In Section IV the models and methods are verified using an experimental dc microgrid set-up. Lastly, in Section V conclusions are drawn.

This work was supported by the framework of the joint programming initiative ERA-Net Smart Grids Plus through the European Union's Horizon 2020 Research and Innovation Programme.

This paper has received funding from the European Union's Horizon 2020 Research and Innovation {rogramme under grant agreement No 734796.

II. Algebraic Model of DC Distribution Systems

Fig. 1 shows an example of a bipolar dc distribution system containing sources, loads and storage. In general, dc distribution systems can be described by their *n* nodes, *l* distribution lines, *o* phase conductors and *m* converters that are connected to the system's nodes.

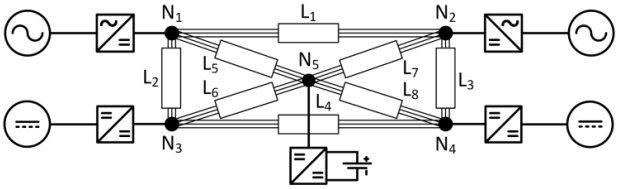

Fig. 1. Example of a dc distribution grid (subsection) containing sources, loads and storage

A. DC Distribution Network Model

A lumped element π model is used for modelling the system's distribution lines. Consequently, the dc distribution system can then be described by the differential equations for the node voltages and line currents, which are given by

$$\boldsymbol{C}\dot{\boldsymbol{U_N}} = \boldsymbol{I_N} - \boldsymbol{\Gamma}^{\boldsymbol{T}}\boldsymbol{I_L} \ , \tag{1}$$

$$\boldsymbol{L}\dot{\boldsymbol{I_L}} = \boldsymbol{\Gamma U_N} - \boldsymbol{R I_L} \ , \tag{2}$$

where the bold face indicates a vector or a matrix. Furthermore, $\boldsymbol{U_N}$, $\boldsymbol{I_L}$, and $\boldsymbol{I_N}$ are the voltages in each node, currents in each line, and the currents flowing from the converters into each node respectively. Additionally, $\boldsymbol{C}$, $\boldsymbol{L}$ and $\boldsymbol{R}$ are the capacitance, inductance and resistance matrices respectively. Moreover, the interconnectivity of the system is described by the incidence matrix, $\boldsymbol{\Gamma}$, which is given by

$$\boldsymbol{\Gamma}(\mathrm{j},\mathrm{i}) = \begin{cases} 1 & \text{if } I_j \text{ is flowing from node } i \\ -1 & \text{if } I_j \text{ is flowing to node } i \end{cases} . \tag{3}$$

where the indices *i* and *j* indicate the nodes and lines respectively. Therefore, I_j is the current flowing in line *j* [18].

B. Converter Model

If it is assumed that the bandwidths of the converters are large enough that they instantaneously react to disturbances in the system, the inner control loops can be neglected and the ideal behavior of converters suffices for modelling [19].

Consequently, all power electronic converters in the system can be represented by either a constant voltage source (for voltage controlling converters), or a constant current source in parallel with an impedance. For example, the currents from droop sources and constant power loads flowing into its node can respectively be described by

$$I_\mathrm{s} = \frac{U_0 - U_i}{Z_s} = I_{s,0} - \frac{U_i}{Z_s} \ , \tag{4}$$

$$I_\mathrm{l} = -\frac{P_l}{U_i} = -\frac{2P_l}{\overline{U}} + \frac{P_l}{\overline{U}^2}U_i = I_{l,0} - \frac{U_i}{Z_l} \ , \tag{5}$$

where U_0 and Z_s are the reference voltage and droop impedance of the droop source respectively. Furthermore, $\overline{U}$ is the voltage at which the constant power load is linearized, and P_l and Z_l are the power and the linearized incremental impedance of the constant power load respectively [20].

The transformation from the ideal circuits to their (linearized) Norton equivalent circuits is shown for droop sources and constant power loads in Fig. 2.

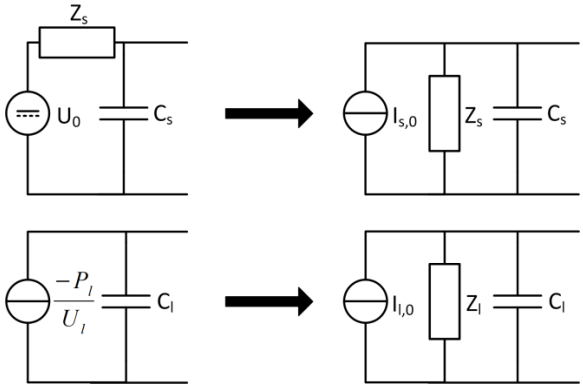

Fig. 2. Ideal and linearized Norton equivalent circuits for droop sources (top) and constant power loads (bottom)

C. DC Distribution System Model

Using (1), (2), and the Norton equivalent for converters (as shown in (4) and (5)) a state-space model of the whole dc distribution system is derived to be

$$\begin{bmatrix}\dot{\boldsymbol{U_N}} \\ \dot{\boldsymbol{I_L}}\end{bmatrix} = \begin{bmatrix}-\boldsymbol{C^{-1}Z^{-1}} & -\boldsymbol{C^{-1}\Gamma^T} \\ \boldsymbol{L^{-1}\Gamma} & -\boldsymbol{L^{-1}R}\end{bmatrix}\begin{bmatrix}\boldsymbol{U_N} \\ \boldsymbol{I_L}\end{bmatrix} + \begin{bmatrix}\boldsymbol{C^{-1}} \\ \emptyset\end{bmatrix}\boldsymbol{I_{N,0}} \ , \tag{6}$$

where $\boldsymbol{Z}$ and $\boldsymbol{I_{N,0}}$ are the impedance and the constant current terms of the Norton equivalent circuits of the converters. Since the impedances of the converters are linearized, this state-space representation also forms a small-signal model.

III. DC Distribution System Stability Analysis

For any system there are two requirements for stability. Firstly, an equilibrium must exist. Secondly, the system must move to the equilibrium and the system's variables must be stable around the equilibrium.

To find the equilibrium the time derivatives of the system are set to zero. Consequently the state variables at the equilibrium can then be found by

$$\begin{bmatrix}\boldsymbol{U_N} \\ \boldsymbol{I_L}\end{bmatrix} = \begin{bmatrix}-\boldsymbol{C^{-1}Z^{-1}} & -\boldsymbol{C^{-1}\Gamma^T} \\ \boldsymbol{L^{-1}\Gamma} & -\boldsymbol{L^{-1}R}\end{bmatrix}^{-1}\begin{bmatrix}\boldsymbol{C^{-1}} \\ \emptyset\end{bmatrix}\boldsymbol{I_{N,0}} \ , \tag{7}$$

Simplifying this equation the node voltages at the equilibrium are derived to be

$$\boldsymbol{U_N} = (\boldsymbol{Z^{-1}} + \boldsymbol{\Gamma^T R^{-1}\Gamma})^{-1}\,\boldsymbol{I_{N,0}} \ , \tag{8}$$

which is equivalent to deriving the equivalent impedance of the network and multiplying it with the constant current terms.

The stability around the equilibrium can be determined by determining the eigenvalues of the left-hand matrix in (6). If and only if all eigenvalues have negative real parts the system will be stable. Moreover, the eigenvalues can be determined by solving

$$\left|\begin{bmatrix}-\boldsymbol{C^{-1}Z^{-1}} & -\boldsymbol{C^{-1}\Gamma^T} \\ \boldsymbol{L^{-1}\Gamma} & -\boldsymbol{L^{-1}R}\end{bmatrix} - \lambda\boldsymbol{I}\right| = \emptyset \ , \tag{9}$$

where $\boldsymbol{\lambda}$ represents the eigenvalues and $\boldsymbol{I}$ is the identity matrix.

A. A Simple DC Distribution System

A simple dc distribution is shown in Fig. 3. This system contains a droop controlled source at node N_1 which is connected to a constant power load at node N_2 via a distribution line. Both are represented by their (linearized) Norton equivalent circuit.

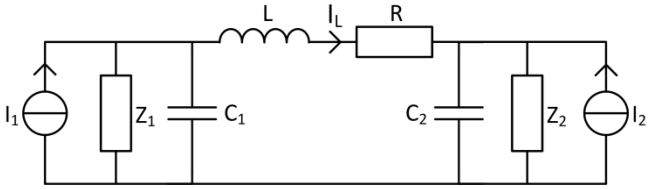

Fig. 3. Simple dc distribution grid with a constant power load (CPL) and a droop source connected via a distribution line.

Utilizing (6), the state-space formulation of this dc distribution system is then given by

$$\begin{bmatrix} \dot{U}_1 \\ \dot{U}_2 \\ \dot{I}_L \end{bmatrix} = \begin{bmatrix} \frac{-1}{Z_1 C_1} & 0 & \frac{-1}{C_1} \\ 0 & \frac{-1}{Z_2 C_2} & \frac{-1}{C_2} \\ \frac{1}{L} & \frac{-1}{L} & \frac{-R}{L} \end{bmatrix} \begin{bmatrix} U_1 \\ U_2 \\ I_L \end{bmatrix} + \begin{bmatrix} \frac{1}{C_1} & 0 \\ 0 & \frac{1}{C_2} \\ 0 & 0 \end{bmatrix} \begin{bmatrix} I_1 \\ I_2 \end{bmatrix}, \quad (10)$$

where it is important to realize that Z_1 is positive and Z_2 is negative (because of the negative incremental impedance of constant power loads).

The characteristic equation for the state-space system can be obtained by utilizing the left-hand side from (9), $|\boldsymbol{A} - \lambda \boldsymbol{I}|$. This characteristic equation is given by

$$\begin{aligned} &\lambda^3 + \lambda^2 \left(\frac{R}{L} + \frac{1}{C_1 Z_1} + \frac{1}{C_2 Z_2} \right) \\ &+ \lambda \frac{1}{L} \left(\frac{L}{Z_1 Z_2} + \frac{R}{Z_1 C_1} + \frac{R}{Z_2 C_2} + C_2 + C_1 \right) \\ &+ \frac{1}{L C_1 C_2} \left(\frac{R}{Z_1 Z_2} + \frac{1}{Z_1} + \frac{1}{Z_2} \right) \end{aligned} . \quad (11)$$

It is required that all coefficients of the characteristic polynomial are positive for it to have poles with negative real parts. To make the conditions not only necessary but also sufficient one additional constraint is required. The product of the second and third coefficient of the polynomial must be greater than the fourth coefficient [21]. Consequently, if the resistance of the line is neglected, the system is stable if and only if

$$|Z_2| > |Z_1| \ , \quad (12)$$

$$C_2 |Z_2| > C_1 |Z_1| \ , \quad (13)$$

$$C_2 + C_1 > \frac{L}{|Z_1||Z_2|} \ , \quad (14)$$

$$\frac{L}{C_2 Z_1 Z_2^2} + \frac{C_2}{C_1 Z_1} > \frac{L}{C_1 Z_1^2 |Z_2|} + \frac{C_1}{C_2 |Z_2|} . \quad (15)$$

A couple of interesting observations can be made from this result.

Firstly, increasing the source's capacitance does not benefit stability as long as the load's capacitance is large enough. On the other hand increasing the load's capacitance is almost always beneficial to stability. This can be explained by realizing that increasing the capacitance of a converter reduces it's time constant. Therefore, increasing capacitance of a dc distribution system without considering the location is not a good practice.

Secondly, increasing inductance always has a negative effect on stability. Even in (15), as long as (12) is adhered to, the inductance has a negative effect on the stability constraint.

B. Complex DC Distribution System

A state-space representation in the form of (6) can also be made for more complex dc distribution systems. Subsequently the coefficients of the characteristic equation can be found utilizing traces of powers or the principal minors of the left-hand matrix utilizing

$$a_1 = 1 \ , \quad (16)$$

$$a_{1+k} = -\frac{1}{k} \sum_{m=1}^{m=k} a_m \mathrm{Tr}(A^{k-m+1}) \, , \quad (17)$$

$$a_{1+k} = (-1)^{-k} \sum \Delta_k \, , \quad (18)$$

where Tr is the trace and Δ_k is the principal minor of A of order k, and A is the left-hand matrix in (6) [22], [23].

Algebraically deriving these coefficients for complex systems results in long equations for each coefficient. However, the results for a few simpler systems confirm the observations from the previous subsection [24].

C. Plug-and-Play DC Distribution Systems

Many applications exist for dc distribution systems with a changing topology and/or participants. Ensuring stability for these plug-and-play system is especially challenging. This is because the incidence matrix for these systems is unknown and therefore deriving and optimizing stability becomes beyond the bounds of possibility.

However, sufficient, but not necessary, requirements can be derived for plug-and-play dc distribution systems. A Brayton-Moser representation of (6) can be used to derive two sufficient conditions for stability. These conditions are

$$P_\Sigma \leq \frac{U_{\min}(U_0 - U_{\min})}{Z_s + R_\Sigma} \ , \quad (19)$$

$$C_i > \frac{\tau_{\max} P_{l,i}}{U_{\min}^2} \ , \quad (20)$$

where P_Σ is the total sum of the consumed power in the system, $U_{\min}$ is the minimum allowed voltage of the system, R_Σ is the total sum of the line resistance in the system, C_i is the output capacitance of the constant power load with power $P_{l,i}$ at node i, and $\tau_{\max}$ is the maximum time constant of the system's lines [20].

Since it is unlikely to have knowledge about the total sum of power and line resistance in the system, (19) can be adhered to by ensuring loads disconnect when the voltage drops below $U_{\min}$. Accordingly, stability is then ensured by sizing the output capacitors of constant power loads by utilizing (20).

IV. Experimental Results

The experimental set-up that is used in this paper is shown in Fig. 3. The laboratory scale microgrid consists of four power electronic converters connected to a dc bus via a line with defined resistance, and inductance. Furthermore, a discharging resistor is connected to the bus to ensure all capacitors are discharged after operation.

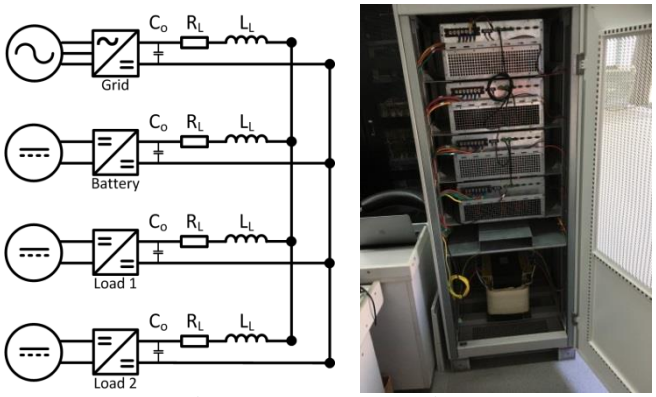

Fig. 4. Schematic (left) and photograph (right) of the DC microgrid set-up consisting of four power electronic converters connected to a dc bus

The four power electronic converters in the microgrid set-up use the topology shown in Fig. 5. The topology consists of three parallel half-bridges that operate, depending on the control, as a three-phase ac/dc converter or a interleaved boost dc/dc converter.

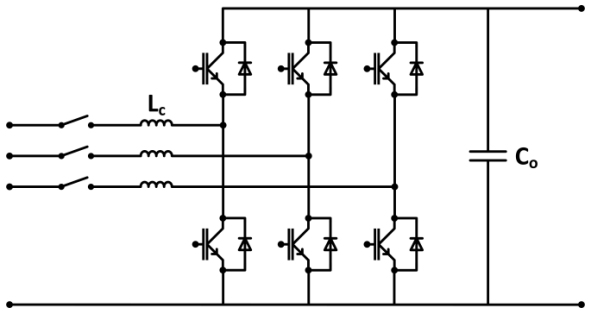

Fig. 5. Topology of the converters that are used in the experimental set-up

For all the experiments three of the converters were operated as dc/dc converters, while one is operated as a grid-connected ac/dc converter (which is connected to the grid via an isolation transformer).

To model the converters a simple average model is used, which are controlled by an inner current control loop and an outer voltage, power or droop control loop. Furthermore, the grid is modelled using (6). The state-space equations of the system are implemented directly via the system's matrices.

A. Modelling Verification

TABLE I. Converter and Line Parameters

Converter	Parameters			
	L_c [mH]	C_o [mF]	R_L [Ω]	L_L [mH]
Grid	1.3	3.0	0.12	1.3
Battery	2.6	1.5	0.08	2.6
PV	2..6	1.5	0.08	2.6
Load	2.6	1.5	0.08	2.6

To verify the combined models of the system and converters an experiment under normal conditions was conducted. The ac/dc converter (labeled "Grid") and a dc/dc converter (labeled "Battery") were operated as power-droop controlled converters. The other two converters operated as constant power converters (labeled "PV" and "Load"). The parameters of the converters and the lines connecting the converters to the bus are given in Table I.

During the experiment several changes in the operating points of the converters were made. First the reference voltage (U_0) of the Grid and Battery is stepped down and later stepped up again. Subsequently, the output powers of the PV and Load converters are changed. The exact scenario is detailed in Table II.

TABLE II. Modelling Verification Scenario

Time [ms]	Control Set Points			
	Grid [U_0]	*Battery* [U_0]	*PV* [P]	*Load* [P]
0.0	380 V	380 V	0	0
1.0	360 V	360 V	0	0
3.0	380 V	360 V	0	0
5.0	380 V	380 V	0	0
7.0	380 V	380 V	3.15 kW	0
9.0	380 V	380 V	3.15 kW	-3.30 kW

The experimental results and the results from simulations for the voltages at each converter's output capacitor are shown in Fig. 6.

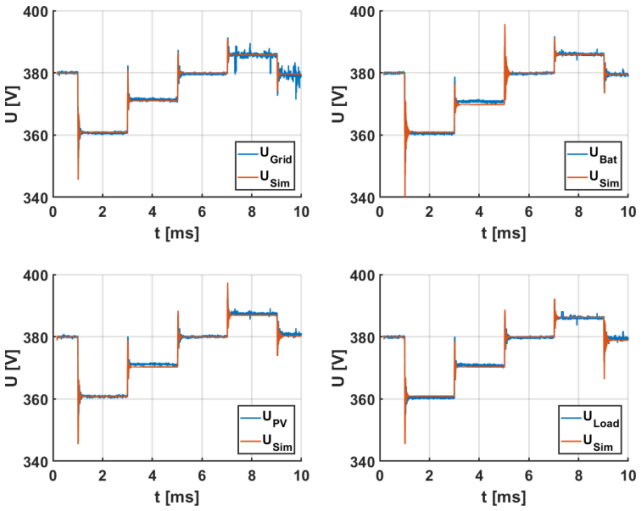

Fig. 6. Simulation and experimental results for the verification of the converter and dc distribution system models

The figures show strong congruency with the simulation models. The experimental results coincide with the simulation results for both the steady state values as well as the peak values during dynamics.

It is important to note that the disturbances on the Grid converter's voltage were caused by nearby activity in the grid, which also reflects to the other converters' voltage.

B. *Equilibrium Instability*

From (12) – (15) it can be seen that, as long as the constant power load has a large enough output capacitance, either a too low or too high droop constant can cause instability. Therefore, in this subsection experiments are conducted to experimentally verify this observation for a more complex system.

For these experiments the Grid tied converter was disconnected from the dc microgrid. This was done to prevent the ac/dc converter to operate in uncontrolled rectifier mode when the voltage drops below 325 V. However, the grid voltage could not drop below 130 V, since the dc/dc converters were fed using a 130 V source. Furthermore, the PV converter was also operated as a constant power load. Additionally, the bus discharge resistance was set at 380 Ω.

First, the Load converter steps up its consumed power from 0 to 2.4 kW. Afterward, the PV converter steps up its consumed power from 0 to 1.6 kW. Furthermore, the Battery converter's reference voltage is set at 380 V. The experimental and simulation results for the Battery converter's output voltage with a droop constant of 26 W/V and 13 W/V are shown in Fig. 7.

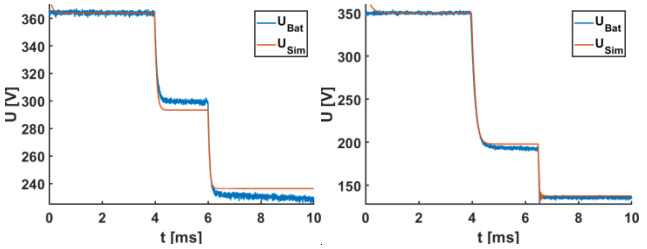

Fig. 7. Simulation and experimental results for the Battery converter's output voltage with a droop constant of 26 W/V (left) and 13 W/V (right)

From Fig. 7 it is clear that the system models follow the experimental results close enough. Furthermore, the system models correctly predict when it becomes unstable. It is seen that when the droop constant becomes too low and the consumed power too high the voltage drops to sharply to zero (or 130 V in this case, since the dc/dc converters' bypass diodes start conducting).

When the droop constant becomes too low the system does not have an equilibrium (or in other words a steady state) and therefore becomes unstable. This instability can also be explained by impedance matching. The droop controlled source supplies its maximum power to the output when the voltage at its output is half the reference voltage. Therefore, if the consumed power forces the output voltage to go below 190 V the source cannot provide the consumed power in the system.

In practical systems this instability can be prevented by disconnecting loads from the system when a certain voltage is reached (assuming that the droop constant cannot be adjusted). For example, in this system the loads must be disconnected before the voltage drops below 190 V to maintain stability. This observation is congruent with the results for the stability of plug-and-play dc distribution systems presented in Section III-C.

C. *Oscillatory Instability*

The experiments for when the droop constant becomes too high are identical to the previous experiments besides a change in droop constant of the Battery converter. The results for the Battery converter's output voltage with a droop constants of 790 W/V is shown in Fig. 8.

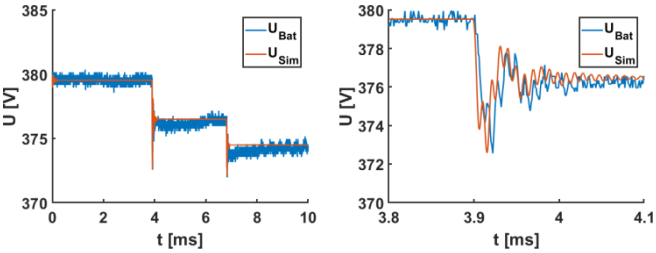

Fig. 8. Simulation and experimental results for the Battery converter's output voltage with a droop constant of 790 W/V

It is again seen that the experimental results follow the simulation results closely even during transients in the system. Although the dc microgrid is stable, the system is becoming somewhat oscillatory, because the damping of the oscillations takes a significant amount of time.

The droop constant of the Battery is further increased to 1050 W/V. The resulting voltage for the Battery converter is shown in Fig. 9.

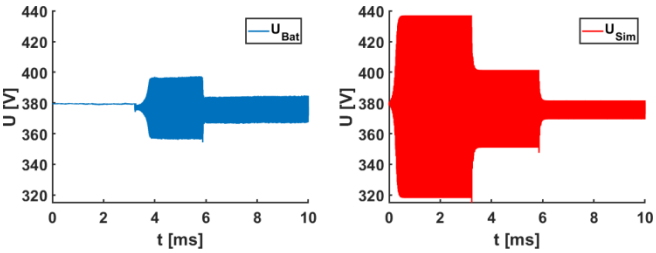

Fig. 9. Simulation and experimental results for the Battery converter's output voltage with a droop constant of 1050 W/V

Although the voltage becomes unstable immediately in the simulations, in the experiment the system only becomes unstable as soon as a transient occurs in the system. However, once the experimental set-up becomes unstable, the frequency and amplitude of the oscillations are correctly predicted by the simulations.

In dc distribution systems oscillations naturally occur in the present CLRC circuits formed by the distribution lines and output capacitors of the converters. Constant power loads enhance these oscillations since they exhibit negative incremental impedance, while droop controlled sources and line resistance provide damping.

The destabilizing factor of constant power loads increase with power consumption, while the damping of droop controlled sources increases with decreasing droop constant. Therefore, when the droop constant is increased too much, the system becomes unstable. If the droop constant is increased the droop source becomes more and more like a constant voltage source, providing no damping to the system.

These observations are again congruent with the results for the stability of plug-and-play dc distribution systems presented in Section III-C.

V. Conclusions

The introduction of renewable energy resources has significant consequences to distribution systems' stability in terms of inertia. Furthermore, the increasing presence of power electronic converters, especially constant power loads, further complicates establishing stable distribution systems.

This paper models dc distribution systems by their node voltages and line currents, while modelling the power electronic converters as their (linearized) Norton equivalent. A state-space representation of the system is created that allows for the analysis of the system's eigenvalues.

Two methods to analyze dc distribution systems' stability are presented. Firstly, the eigenvalues of the state matrix can be determined either directly or via determining the coefficients of the characteristic equations. Secondly, a Brayton-Moser representation of the system can constructed to arrive at sufficient conditions for plug-and-play systems.

The models and algebraic methods were verified using an experimental dc microgrid set-up. The models showed strong congruency with the microgrid behavior. Furthermore, the experiments confirmed that the instability of dc distribution systems can be classified in two categories; equilibrium instability and oscillatory instability. Equilibrium instability occurs when the system does not have an equilibrium, and can be caused by a droop constant that is too low. Oscillatory instability occurs when oscillations are not damped sufficiently, and can be caused by a droop constant that is too high.

In the future the presented analytical methods can be used to analyze, optimize and/or ensure the stability of dc distribution systems. Furthermore, a focus can be made on preventing the two distinct forms of instability while designing a dc distribution system.

References

[1] J.-C. Kim, S.-M. Cho, and H.-S. Shin, "Advanced power distribution system configuration for smart grid". IEEE Transactions on Smart Grid, vol. 4, no. 1, 2013.

[2] L. Mackay, T. Hailu, L. Ramírez-Elizondo, and P. Bauer, "Towards a DC distribution system: Opportunities and challenges". In Proceedings IEEE 1st International Conference DC Microgrids (ICDCM), 2015.

[3] N. Hatziargyriou, H. Asano, R. Iravani, and C. Marnay, "Microgrids". IEEE Power & Energy Magazine, vol. 5, no. 4, Jul. 2007.

[4] F. M. F. Flaih, X. Lin, M. K. Abd, S. M. Dawoud, Z. Li, and O. S. Adio, "A new method for distribution network reconfiguration analysis under different load demands". Energies, vol. 10, no. 4, 2017.

[5] D. M. Larruskain, I. Zamora, O. Abarrategui, and Z. Aginako, "Conversion of AC distribution lines into DC lines to upgrade transmission capacity". Electrical Power System Research, vol. 81, no. 7, 2011.

[6] T. Hakala, T. Lähdeaho, and P. Järventausta, "Low-voltage DC Distribution: Utilization potential in a large distribution network company". IEEE Transactions on Power Delivery, vol. 30, no. 4, 2015.

[7] Ghareeb, A.T.; Mohamed, A.A.; Mohammed, O.A. "DC microgrids and distribution systems: An overview". In Proceedings of the 2013 IEEE Power & Energy Society General Meeting.

[8] Patterson, B.T. DC, Come Home: DC Microgrids and the Birth of the "Enernet". IEEE Power & Energy Magazine, 2012, 10.

[9] Planas, E.; Andreu, J.; Garate, J.I.; de Alegria, I.M.; Ibarra, E. "AC and DC technology in microgrids: A review". Renewable Sustainable Energy Reviews, 2015, 43.

[10] Driesen, J.; Visscher, K. "Virtual synchronous generators". In Proceedings of the 2008 IEEE Power and Energy Society General Meeting.

[11] Bottrell, N.; Prodanovic, M.; Green, T.C. "Dynamic Stability of a Microgrid With an Active Load". IEEE Transactions on Power Electronics, 2013, 28.

[12] Cespedes, M.; Xing, L.; Sun, J. "Constant-Power Load System Stabilization by Passive Damping". IEEE Transactions on Power Electronics, 2011, 26.

[13] Dragicevic, T.; Lu, X.; Vasquez, J.C.; Guerrero, J.M. "DC Microgrids - Part I: A Review of Control Strategies and Stabilization Techniques". IEEE Transactions on Power Electronics. 2016, 31.

[14] Sanchez, S.; Molinas, M. "Degree of Influence of System States Transition on the Stability of a DC Microgrid". IEEE Transactions on Smart Grid 2014, 5.

[15] Riccobono, A.; Santi, E. "Comprehensive Review of Stability Criteria for DC Power Distribution Systems". IEEE Transactions on Industrial Applications, 2014, 50.

[16] Makrygiorgou, D.I.; Alexandridis, A.T. "Stability Analysis of DC Distribution Systems with Droop-Based Charge Sharing on Energy Storage Devices". Energies 2017, 10.

[17] Shamsi, P.; Fahimi, B. "Stability Assessment of a DC Distribution Network in a Hybrid Micro-Grid Application". IEEE Transactions on Smart Grid 2014, 5.

[18] N. H. van der Blij, L. M. Ramírez-Elizondo, M. T. J. Spaan, and P. Bauer, "A state-space approach to modelling DC distribution systems". IEEE Transactions on Power Systems, vol. 33, no. 1, 2018.

[19] A. Emadi, A. Khaligh, C. H. Rivetta, and G. A. Williamson, "Constant power loads and negative impedance instability in automotive systems: Denition, modeling, stability, and control of power electronic converters and motor drives". IEEE Transactions on Vehicle Technology, vol. 55, no. 4, 2006.

[20] N. H. van der Blij, Nils, L. M. Ramirez-Elizondo, M. T. J. Spaan, P. Bauer, "Stability and Decentralized Control of Plug-and-Play DC Distribution Grids". IEEE Access, 2018.

[21] Barnett, S.; Šiljak, D, "Routh's algorithm: A centennial survey". SIAM Rev. 1977, 19.

[22] Zadeh, L.; Desoer, C. "Linear System Theory: The State Space Approach". McGraw-Hill Series in System Science, McGraw-Hill: New York, 1963.

[23] Mirsky, L. "An Introduction to Linear Algebra". Dover Books on Mathematics, Dover Publications: New York, 2012.

[24] van der Blij, Nils; Ramirez-Elizondo, Laura; Spaan, Matthijs; Bauer, Pavol, "Stability of DC Distribution Systems: An Algebraic Derivation". Energies, 2017.